Piriyanth Sakthithasan *
Luisa Orth
Maximilian Venhuis
Norbert Kockmann

Design of a Process-Intensified Liquid-Liquid Extraction Cell for Higher Temperature and Pressure

Liquid-liquid extraction is performed in most cases at moderate temperatures to utilize its energy-efficient advantages. A new concept of a process-intensified extraction device for liquid-liquid systems at increased temperature and pressure is presented. The design of the extraction device with its new subsystems, such as stirrer and pulsation, including a safety concept, is discussed within this work. Further, a mechanical stability analysis is shown to prove the usability of the extraction device for increased temperature and pressure.

Supporting Information available online

Keywords: High-pressure extraction, Liquid-liquid extraction, Process intensification, Solvent extraction, Stirred-pulsed extraction

Received: November 08, 2022; *revised:* December 14, 2022; *accepted:* January 13, 2023

DOI: 10.1002/ceat.202200550

1 Introduction

Current trends in the process industry lead to the production of more and more customer-defined higher-value specialty chemicals [1]. This transition to specialty chemicals results in challenges in the process development. First insights can be gained in time-consuming and costly laboratory-scale studies. Miniaturized devices like microreactors for reactions and miniaturized separation methods come in handy to gain first insights in a small scale and overcome the time-consuming and costly efforts [2].

In the area of separation methods, thermal separation methods are the most commonly used methods to purify a fluid stream in the process industry [3]. Here, liquid-liquid extraction, also called solvent extraction, is one of the most energy-efficient thermal separation methods [4]. Due to the flexibility of liquid-liquid extraction, a broad range of application from biomedical [5] to pharmaceutical [6] and also in the battery [7] industry is possible. Usually, the extraction is performed under environmental conditions and provides a high separation efficiency while offering a high throughput [4].

At the Laboratory of Equipment Design, the stirred-pulsed DN15 extraction measurement cell has been developed [8, 9]. It combines the low effort of miniaturized devices with the high efficiency of liquid-liquid extraction. Process intensification concepts are applied by introducing stirring and pulsation to achieve a higher separation efficiency while offering a high maximum throughput [8, 9]. Other approaches for process intensification are, for example, by introducing reactive components [10], using centrifugal contractors [11], or scaling down the extraction device to the microfluidic level [12]. Microfluidic devices utilize the high surface-to-volume ratio to gain a high extraction efficiency [13].

The phase separation can be realized using differently coated channels but does not offer high throughput as columns [14, 15]. On the other side, centrifugal contactors such as the centrifugal partition chromatography (CPC) or the annular centrifugal contactor/extractor (ACC/E) allow a higher throughput but are also sensitive to their setup [15]. CPC utilizes a rotating disc containing multiple connected cascading chambers [16]. ACC/E has a different experimental setup but also employs the introduced rotational forces. It utilizes an inner rotating and an outer static cylinder [17]. Due to a gap between both cylinders, the light and the heavy phase can be introduced. Due to the rotational forces the phases can be separated and collected. It allows like the CPC a high throughput and extraction efficiency [18]. Although there are a vast majority of extraction devices with high throughput and extraction efficiency available, none of these considered increasing temperature and pressure.

An extraction device for increased temperature and pressure could lead to even higher separation efficiencies, as literature showed higher diffusion rates at elevated temperatures [19–21]. The physical properties also change at higher temperature and pressure. In literature, it has been reported that viscosity can influence mass transfer during solvent extraction [22]. Especially high-viscous systems are limited in mass transfer [22]. The density also changes at elevated temperatures, resulting in the change of, e.g., the ascent speed of the droplets [23]. This speed change could probably lead to varying residence times of

Piriyanth Sakthithasan https://orcid.org/0000-0002-2759-2988,
Luisa Orth, Maximilian Venhuis,
Prof. Dr.-Ing. Norbert Kockmann
https://orcid.org/0000-0002-8852-3812
(piriyanth.sakthithasan@tu-dortmund.de)
TU Dortmund University, Department of Biochemical and Chemical Engineering, Laboratory of Equipment Design, Emil-Figge-Strasse 68, 44227 Dortmund, Germany.

the disperse phase compared to experiments at ambient conditions.

Another significant parameter is that the interfacial tension strongly depends on the operating temperature [24, 25]. With this strong dependency, it is possible to adjust the interfacial tension of the used substance system. Consequently, the combination of these aforementioned effects could lead to an improvement in extraction performance.

Existing concepts of liquid-liquid extraction at increased temperature and pressure do not utilize combined energy inputs such as stirring and pulsation. Pressurized liquid extraction is an existing application of elevated pressure and temperature in solid-liquid extraction at subcritical pressure and temperature [26]. Here, batch operations are performed to extract bioactive compounds from natural resources, hence, mainly in use for sample preparation in analytical chemistry [27] or phytoextraction of plant-based pharmaceuticals [28].

The corresponding apparatus are operated in batch and consist primarily of a cylindrical extraction cell and a pump to build up the pressure. There are additional components such as purging gas and a backpressure valve to maintain a stable operation. The primarily solid sample will be prepared for extraction in the extraction cell. Its application is mainly in the analytical field. To perform the extraction continuously, it will be performed in a continuously flown extraction cell maintained at the increased process conditions. The phase separation will then occur after cooling the fluids at ambient conditions. In summary, the devices for pressurized liquid extraction do not utilize the concept of process intensification but their concepts can be used for developing a process-intensified extraction device [29].

Another extraction approach at increased temperature and pressure is the supercritical extraction with carbon dioxide [30]. As the name suggests, the extraction is performed at supercritical conditions of the fluids. They are mostly used to extract natural compounds [31]. In this case, continuous operation with spray, sieve tray, or packed column can be realized [32, 33]. In these setups, supercritical carbon dioxide is transported from a supply tank to the extraction device. Although the target operating conditions of the new extraction device will be below the supercritical level, existing concepts like the design of the device [34, 35] or control concepts [36] can be adapted for the design.

In this contribution, an extended design of the stirred-pulsed extraction is presented. This new concept is designed for increased temperature and pressure. First, the design methodology is explained. Then the design of the extraction plant, which consists of the extraction device itself and various subsystems, is presented. Finally, a stability analysis of the extraction device in FEM analysis by ANSYS Mechanical is described.

2 Design Methods

The design of the high-pressure concept has been developed according to the guideline of the VDI 2220–2223. It subdivides the design of the extraction device into four phases: analysis, conceptualization, design, and elaboration of the first design [37–40]. The computer-aided design (CAD) software Autodesk Inventor® (Autodesk, San Rafael, CA, USA) has been used for the mechanical design of the extraction device.

After finishing the design, the next step is verifying pressure stability and strength. Though preliminary studies show a slight pressure difference (±20 kPa) during the pulsation, structural analysis has been performed for static loads in ANSYS Mechanical 2021R1 (ANSYS Inc., Canonsburg, PA, USA). With the results of the simulated data, the realized safety factor S_{real}[1)] can be determined as the ratio of the maximum von-Mises stress in the device and the yield strength R_e of the material. According to the ASME standards, pressure vessels need a safety factor of at least 3.5 [41].

Using these methods, the design of the extraction device and its internal components is carried out and verified regarding its application. Since the extraction device allows for operation at elevated process conditions, auxiliary devices must be identified and specified for the increased process conditions. Therefore, a control concept and piping and instrumentation diagram have been developed for this process and validated against pressure stability.

3 Extraction Plant Design

The final design of the high-pressure measurement cell can be separated into multiple stages. The first and most important stage is the design of the extraction devices main body. The second and third stages are the layout for energy inputs, the stirring and pulsation, within the extraction device. Finally, the last stage deals with maintaining the increased temperature and pressure within the extraction device. The overall design of the extraction device is similar to previous designs of the extraction measurement cell [9].

3.1 Extraction Device Design

The design of the extraction device is depicted in Fig. 1, whereas some of the characteristic dimensions are listed in Tab. 1. Additional information is provided in the Supporting Information.

The in- and outlets for the mass flows are placed nearly identical to existing designs [9]. The inlet for the light phase (6), the heavy phase (7), and the outlet for the extract phase (3) are at the same position. The outlet for the raffinate phase (4) is switched to the right side of the extraction device. The design of the ports mainly follows a route from the left (inlets) to the right (outlets) to gain a more structured setup. Because the device is designed to operate at elevated pressure levels, the top of the device needed to be closed off from the environment. A magnetic coupling (1) (MINEX SA 22/4, KTR-Kupplungstechnik GmbH, Rheine, Germany) has been integrated to accomplish this task.

The active extraction section is divided into six compartments with the same arrangement and design for the spacers (10), stirrer modules (11), and sieve trays (12). The pulsation connection (5) is placed at a lower position to prevent the pul-

1) List of symbols at the end of the paper.

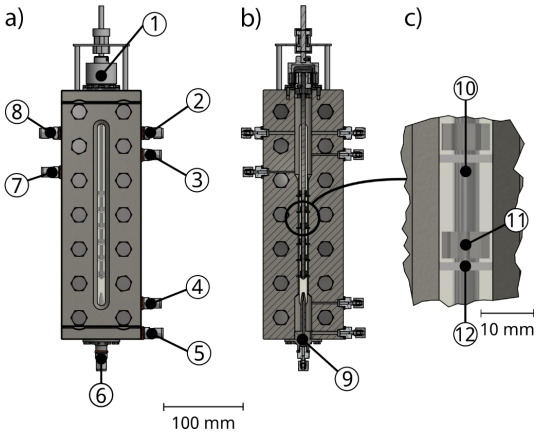

Figure 1. Assembled view of the extraction device (a) with a cross-sectional cut (b) and a close-up of one stirred cell (c).

Table 1. Geometric properties of the designed extraction device.

Property	Existing measurement cell design [9]	New measurement cell design
n_{comp} [–]	6	6
A_{active} [mm^2]	167.79	144.94
h_{active} [mm]	136	124
V_{active} [mL]	19	18

sation from directly influencing the disperser (9). Due to the pressurization of the extraction device, an inlet (8) and outlet (2) for the pressurization gas is added to the extraction device.

Since the operation at elevated pressure does not allow for glass as column material, the optical accessibility to evaluate the experiments must be realized. To counteract the loss of optical accessibility of metal, longitudinal sight glasses (4) (DIN 7081, MAXOS, Auer Lightning GmbH, Bad Gandersheim, Germany), according to DIN7081, have been added to the front and the back of the extraction device. A cross-sectional sketch of this setup is displayed in Fig. 2. In this design, both

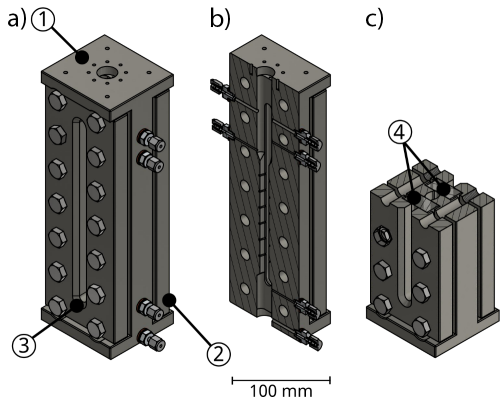

Figure 2. Isometric view of the extraction device without stirrer system and disperser in full (a) and cross-sectional viewpoints (b, c).

sight glasses (4) are clamped with front (3) and back (2) plates at the main body (1). The field of view is limited to 10 mm, as the clamping mechanism for the sight glasses needs an increased mounting surface.

With the introduction of the longitudinal sight glasses, the most process significant change is the shape of the active extraction area. Fig. 3 shows the assembled cross-sectional view of the new design and a comparison of the active extraction area of the existing design and the new proposed design.

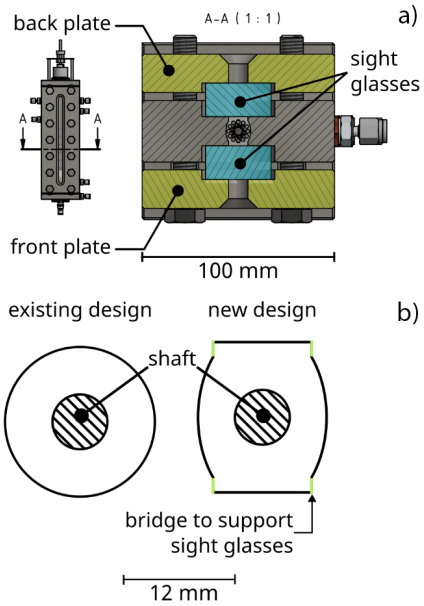

Figure 3. Cross-sectional view of the extraction device (a) with a comparison (b) of the existing and new designs active extraction area.

Due to the longitudinal sight glasses, the round cross section of the previous design has not been maintained, as indicated in Fig. 3b. Although these bridges could possibly lead to dead zones, they are mandatory to support the longitudinal sight glasses as these are pressed via the front and back plate to the main body (see Fig. 3a).

Detailed information regarding the design of the sealing and internals can be found in the Supporting Information.

3.2 Design of the Subsystems

Most parts of the extraction device design are illustrated in the previous Sect. 3.1. Subsystems such as the stirrer system, the pulsation unit, and the temperature control (see the Supporting Information) needed special attention. As the fume hood already provides a facility to control the pressure via nitrogen, pressure control does not need any special attention.

3.2.1 Stirrer System

As the substance system within the extraction device needs to be stirred, a stirrer system has to be implemented. Due to

increased pressure, the stirring cannot be realized by introducing a stirrer shaft as in the previous design [9]. An adequate sealing method is needed to prevent leakage. Here, a magnetic coupling (MINEX SA 22/4, KTR-Kupplungstechnik GmbH, Rheine, Germany) is used to fulfill this task. It consists of an external rotor, an internal rotor, and a containment shell. The containment shell is needed to separate the pressurized fluids in the extraction device from the environment and allows for generating a pressurized environment. The top assembly with a stabilizing setup is displayed in Fig. 4.

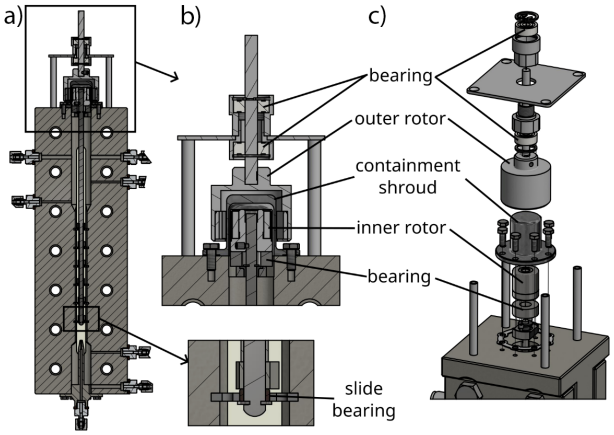

Figure 4. Cross-sectional close-up (a) and (b) of the stirrer system and the corresponding assembly to stabilize the inner rotor, including the stirrer shaft. Explosion view (c) of the outer stirrer assembly with the corresponding inner/outer rotor and containment shroud.

This setup allows for dispersing the fluids while the extraction device can be operated at increased pressure. The following subsection describes the extraction device's pulsation system, the second energy input.

3.2.2 Pulsation System

The design of the pulsation unit is carried out based on the same guidelines as the main body of the extraction devices. A pneumatic cylinder (ADN-63-5-I-P-A, Festo SE & Co. KG, Esslingen, Germany) in combination with a pressure transducer is selected as the pulsation mechanism. By selecting EPDM seals, initial test series are conducted with the possible substance mixtures. As the pulsation of the liquid phase will lead to pressure fluctuations during the extraction process, a back coupling to the pressurized gas phase of the extraction device has been integrated. Including a buffer tank between the gas phase of the measurement cell and the pulsation unit also protects the seals from rising solvent vapors.

To enable automatic operation, the manually adjustable throttle check valves are replaced by controllable proportional control valves. Calculations of the stroke times, stroke speeds, and volume flow within the pneumatic cylinder are the basis for selecting the proportional control valves (PVQ13, SMC Deutschland GmbH, Egelsbach, Germany). The material 1.4571 is used to construct the buffer tank, the pressure transducer, and the piston rod extension. The design of the overall system is depicted in Fig. 5.

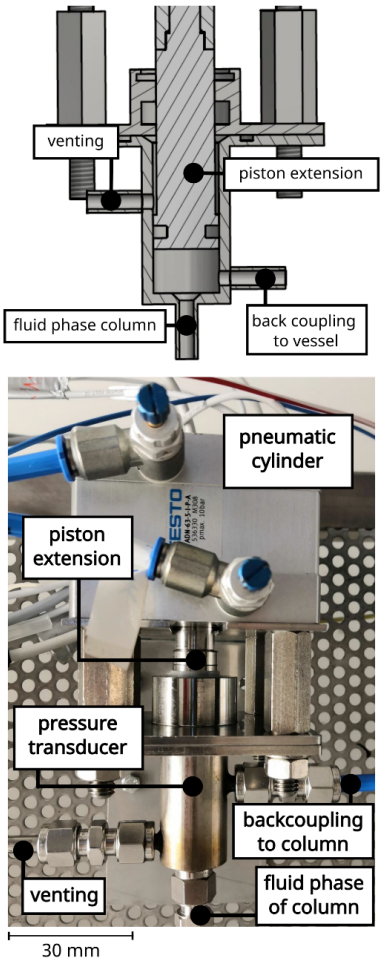

Figure 5. CAD design of the pulsation unit without the pneumatic unit at the top and image of the finished pulsation unit, including the pneumatic unit.

The proportional control valves also make it possible to adjust the stroke speed by setting an appropriate flow rate. Automatic operation can be realized by selecting preset stroke times. With the help of the proportional control valves, it is possible to approach various pulsation profiles [42] up to a frequency f of 0.625 Hz independent of the pressure inside the extraction device. By monitoring the pressure inside the measurement cell and the compressed air line, pressure fluctuations can be detected, and the operation of the pulsation unit can be adjusted.

3.2.3 Safety Measures and Piping and Instrumentation Diagram

Multiple safety concepts have been developed to allow a safe operation at increased temperature and pressure. Based on the selected components, a piping and instrumentation diagram (P&ID) is created. The resulting P&ID is displayed in Fig. 6.

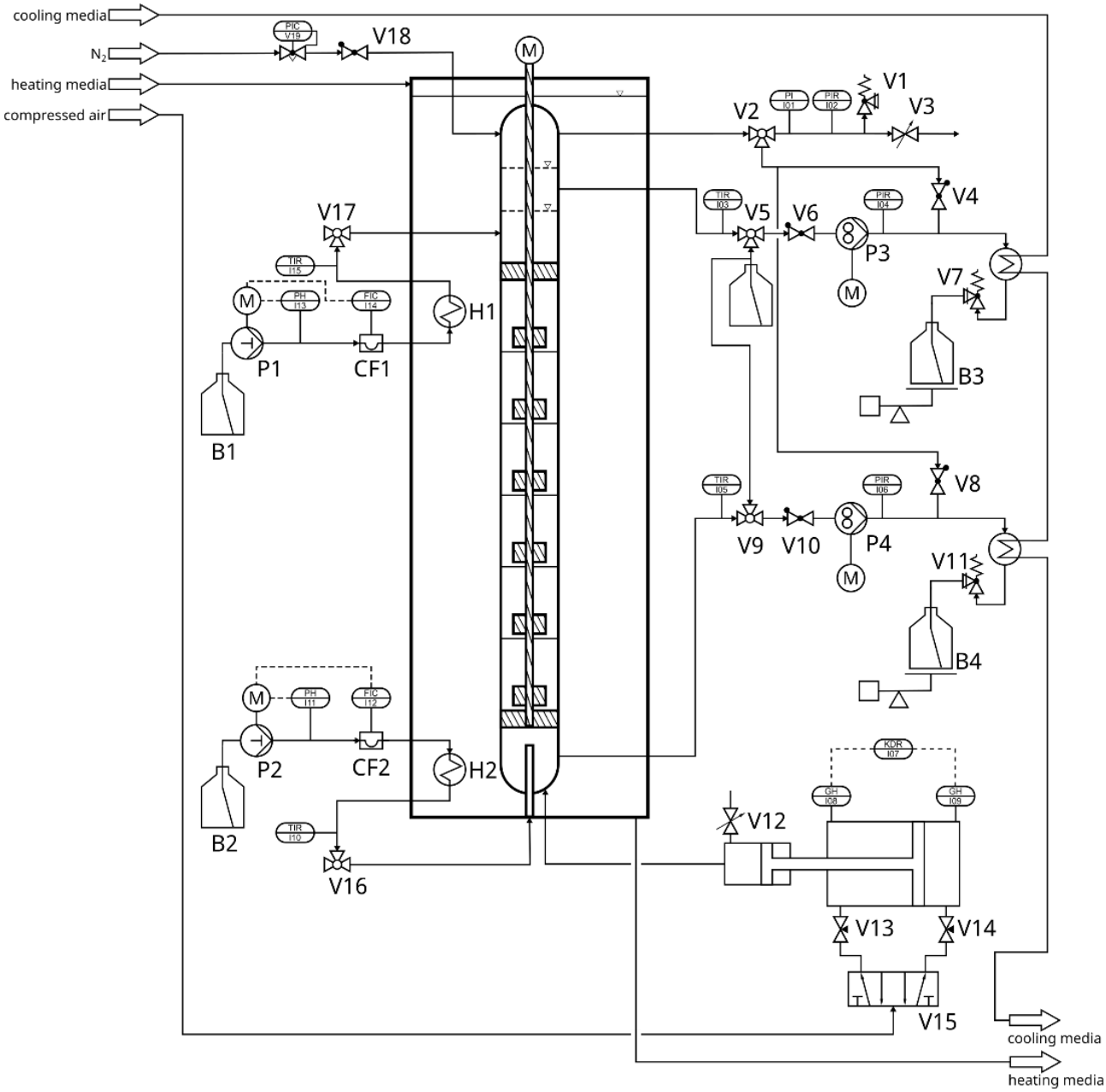

Figure 6. Piping and instrumentation diagram of the final extraction plant with the ingoing streams on the upper left and the outgoing streams at the lower right.

The pressure is built with nitrogen and adjusted via the pressure regulator 16. The overall safety concepts utilize spring-loaded valves V7 and V11 (RV Series, Hy-Lok D Vertriebs GmbH, Oyten, Germany) at the outlets and safety integrations within the pump systems, P1 and P2, preventing overpressure at the inlets. A pressure regulator at the gas inlet avoids generating overpressure by nitrogen. Multiple pressure sensors are integrated into the piping to observe the pressure at each piping segment. With this concept, a safe operation of the plant is possible. The ongoing chapter will now discuss the mechanical studies performed to evaluate the pressure stability of the extraction device.

4 Mechanical Stability Analysis

In this section, the static analysis of the main body of the extraction device is discussed. All static analyses are performed on ANSYS 2021R1. Tab. 2 lists the materials and their mechanical properties. The materials have been selected based on the prior experience of the mechanical workshop at the TU Dortmund University and their chemical resistance.

Table 2. Material properties used in the mechanical stability analysis within ANSYS 2021 R1 [43].

Material	R_m [MPa]	R_e [MPa]
AISI 304L, annealed (1.4306)	5.327×10^2	2.020×10^2
AISI 316L, annealed (1.4404)	5.212×10^2	2.296×10^2
AISI 316Ti, annealed (1.4571)	5.758×10^2	2.437×10^2

4.1 Model Setup

In the next step, the numerical mesh is generated. Therefore, the geometric model has been prepared according to Sect. S4 in the Supporting Information. Due to the complexity of the design, an unstructured mesh is used. A short overview of the mesh is given in Tab. 3.

Table 3. Overview of the generated mesh with the number of elements/nodes and their sizes in ANSYS Mechanical.

Parameter	Value
n_{nodes} [–]	719 405
$n_{element}$ [–]	494 068
$s_{element,\,default}$ [m]	2.5×10^{-3}
$s_{element,\,refined}$ [m]	1.0×10^{-3}

The standard element size is set to 2.5×10^{-3} m. Additional refinement is performed at the pressure-induced areas, such as the inner body and the fluidic connections. Moreover, the bridge at which the longitudinal glass stays is refined, as preliminary studies showed increased stress in this area. The element size at the refined area is at 1.0×10^{-3} m. Images of the generated mesh and the refined bridge are given in Figs. S7 and S8 in the Supporting Information. The mesh quality has been evaluated using the orthogonality and the aspect ratio, as indicated in Sect. S5 of the Supporting Information. Based on the ANSYS Meshing Guidelines, the overall mesh quality has been determined as sufficient.

To provide a largely accurate representation of the real environment, boundary conditions are used. At first, pressure loads are applied to the inside areas of the extraction device and the fluidic paths. The pressure load is varied with the material to perform a design study. The bottom of the extraction device has been set as fixed. The mounted, longitudinal sight glasses are modeled via a displacement condition. As the sight glasses are clamped to the surfaces, a displacement along the normal of the mounting surface is not possible and can be set to zero. The clamping mechanism of the sight glasses consists of 14 M12 screws, which need to be mounted through holes. Consequently, the screws will prevent the movement of the holes along the radial and tangential directions. Based on these boundary conditions, a mechanical study is performed. A detailed image of the applied boundary conditions is given in Sect. S6 of the Supporting Information.

4.2 Static Analysis Results

The results of the mechanical study are presented in Fig. 7. Since the tubing and the connectors are rated for up to 20.0 MPa(g), the simulations are also performed until 20.0 MPa(g). The simulations are performed for the three materials listed in Tab. 2. Detailed images of the stress regions (Figs. S9 and S10) are presented with numerical values in Tab. S3.

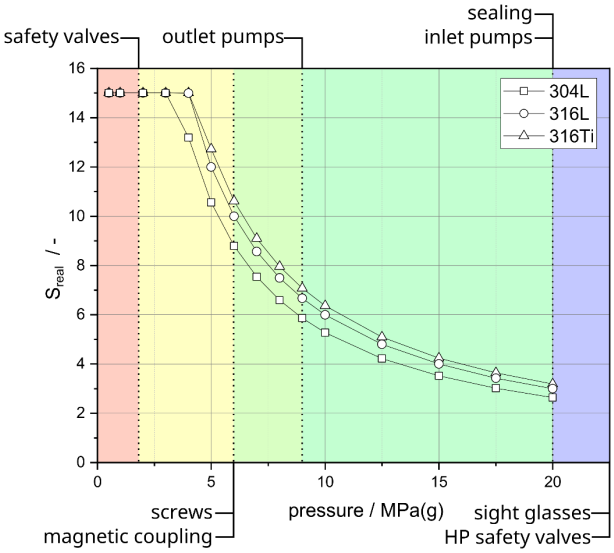

Figure 7. Realized safety factor S_{real} in dependency of the pressure inside the extraction device combined with the used components for the plant design.

All the materials are suitable for the extraction device up to a pressure of 12.5 MPa(g). Increasing the pressure to 15.0 MPa(g) results in getting close to the safety limits for the material 304L. At a pressure of 17.5 MPa(g), all the materials, despite 316Ti undershoot the limit of the safety factor. In summary, all materials can be used for the extraction device up to a pressure of 15.0 MPa(g). When comparing the materials with each other, 316Ti performed best. This behavior can be explained by the high tensile yield strength of 316Ti, as indicated in Tab. 2. Since 316Ti outperformed all the other materials and the mechanical workshop at the TU Dortmund University has the best experience with processing the material, 316Ti is chosen for the extraction device material.

The result of the mechanical study is then combined with the limitations of the used components. This results in colored areas in Fig. 7 describing the overall plant's pressure-based operation area. At first glance, the safety valves with a maximum operating pressure of 1.72 MPa(g) seem to be the weakest component in the presented design. Since preliminary experiments are planned to be performed at low pressure, the safety valves can be changed to a high-pressure (HP) version later. These valves can then be operated up to 41.4 MPa(g). Although most components and the extraction device are rated for higher pressure levels, the experiments are limited to 6.0 MPa(g). This is caused by the mechanical limitation of the magnetic coupling provided by the manufacturer. Due to this limitation, the

screws for the clamps and the magnetic coupling are also designed for 6.0 MPa(g).

5 Preliminary Study

After verifying the mechanical stability, a preliminary study is performed with the designed setup. An image of the used setup is displayed in Fig. 8.

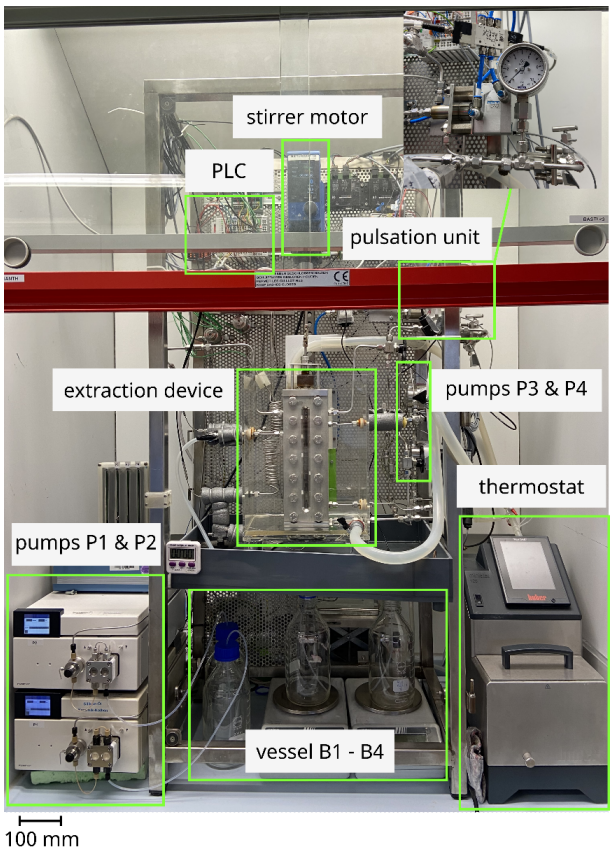

Figure 8. Overview of the built extraction plant. Pumps P1 and P2 transport the heavy and light phases from B1 and B2 into the extraction device. P3 and P4 transport the outgoing streams into B3 and B4. The thermostat is used to control the temperature during the extraction.

In this preliminary study, the load limit B_{Flood} and the extraction performance N_{th} have been investigated. The load limit can also be described as the maximum throughput of the extraction device. The procedure for determining the parameters is analogous to the experiments performed in the existing design [9]. The experiments are performed with the EFCE (European Federation of Chemical Engineering) test system water (deionized, electrical conductivity $\leq 5\times10^{-4}\,\mathrm{S\,m^{-1}}$), acetone (> 99.8 %, VWR Chemicals, Germany), and *n*-butyl acetate (> 99.5 %, Merck KGaA, Germany). The system has a medium surface tension ($\sigma = 13.96\times10^{-3}\,\mathrm{N\,m^{-1}}$) [19] and has shown a good response to the stirred-pulsed extraction [4, 9]. The mass transfer has been performed from the continuous heavy phase (DI water) to the dispersed light phase (*n*-butyl acetate). Therefore, the feed (water and acetone) has been dissolved with 5 wt % of the solute (acetone) and then contacted with the pure solvent (*n*-butyl acetate). The results of this study are illustrated in Fig. 9.

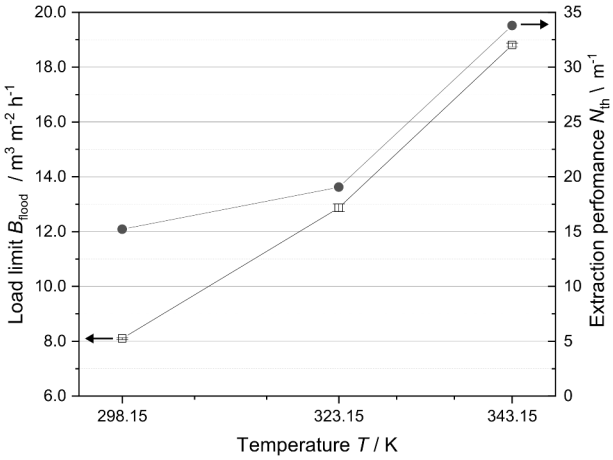

Figure 9. Preliminary study of the extraction at increased temperature and pressure at T = 298.15 K, 323.15 K, and 343.15 K. The mass transfer experiments have been performed at 0.3 MPa(g), n_{stirrer} = 700 rpm, and f = 0.5 Hz.

The load limits have been determined without acetone. Overall, an increase in the load limit can be observed with rising temperature. The load limit increases from 8.1 to 18.8 $\mathrm{m^3 m^{-2} h^{-1}}$. Multiple phenomena like changing interfacial tension or density, thus ascending speed, could raise the load limit. Here, it is visible that an increasing temperature leads to a higher throughput. A detailed investigation of the substance parameters is needed to understand the physical phenomena.

As described, the experiments have been performed at a constant pressure of 0.3 MPa(g) to prevent evaporation of the solute acetone. The device has been operated at 80 % of the load limit determined beforehand to allow a stable operation. The number of theoretical stages has been calculated via the McCabe-Thiele methods and corresponding simulated (UNIFAC LLE) equilibrium data (Aspen Plus V12, Aspen Technology Inc., Bedford, USA).

The extraction performance shows similar rising trends as the load limit. An increase from 15.2 to 33.8 $\mathrm{m^{-1}}$ stages has been overserved during an increase of 50 K. A reason for this behavior could be the increasing diffusion rates [19]. Another reason could be the increased throughput within the extraction device. This higher throughput could result in the accumulation of the disperse phase, therefore extracting a higher amount of the solute. Future experiments will give more detailed information on the separation performance at elevated pressure and temperature.

6 Conclusion

An existing design of a DN15 measurement cell has been transferred to a high-pressure concept. Therefore, an overall plant concept needed to be created. In the first step, the DN15

measurement cell is redesigned. With this redesign, an improved sealing system and redesigned internals have been introduced. With the introduction of increased temperature and pressure, multiple subsystems are revised. A new stirrer and pulsation system are designed to allow the operation at higher temperatures and pressure. A temperature control system is also designed to maintain the process temperature and cool the outgoing stream later. In the last step, the mechanical stability of the new extraction device has been verified in ANSYS Mechanical and summarized with the stability of the other components of the design.

With this overall plant design, possible studies can be performed at increased pressure and temperature. Separation tasks with low-boiling components such as methanol can be performed at elevated temperatures by applying higher pressure. Furthermore, the stirred-pulsed extraction can also be integrated into processes with higher operating pressure without reducing pressure; thus, energy can be saved. A separate experimental verification needs to be performed before operating at the simulated pressure levels.

A preliminary study has been performed to show the possibilities of the new extraction device. With slight elevation of the process temperature, the overall throughput and extraction performance have been increased. Evaporation of the solute has been prevented by performing the extraction at a higher pressure level. In order to gain more insights, detailed studies need to be carried out with this new design. Even more substance data has to be gathered to understand the underlying phenomena during the extraction. Effects like changing surface tension, density, and viscosity are some factors that need to be determined.

Supporting Information

Supporting Information for this article can be found under DOI: https://doi.org/10.1002/ceat.202200550. This section includes additional references to primary literature relevant for this research [44–46].

Data Availability Statement

The data that supports the findings of this study are available in the supplementary material of this article.

Acknowledgment

The authors acknowledge financial support by Deutsche Forschungsgemeinschaft and TU Dortmund University within the funding program Open Access Costs. We would like to thank our technician Carsten Schrömges and the support from the mechanical workshop. The authors also would thank the people from Frenzelit for the technical support and the networking program "Sustainable Chemical Synthesis 2.0" (SusChemSys 2.0) for the support and fruitful discussions across disciplines. Open access funding enabled and organized by Projekt DEAL.

The authors have declared no conflict of interest.

Symbols used

A	[m^2]	area
B	[$m^3m^{-2}h^{-1}$]	load
f	[Hz]	frequency
h	[m]	height
n	[–]	number
Re	[MPa]	yield strength
R_m	[MPa]	tensile strength
s	[m]	length
S	[–]	safety factor
T	[K]	temperature
V	[mL]	volume

Greek letters

σ	[N m^{-1}]	surface tension
σ_v	[MPa]	von-Mises stress

Sub- and superscripts

active	active
comp	compartment
element	elements in mesh
element, default	default elements in mesh
element, refined	refined elements in mesh
flood	flooding
max	maximum
nodes	nodes in mesh
real	realized
rel	relative
stirrer	stirrer
th	theoretical

Abbreviations

ACC/E	annular centrifugal contactor/extractor
CAD	computer-aided design
CPC	centrifugal partition chromatography
DI	deionized
DN	diameter nominal
EFCE	European Federation of Chemical Engineering
FEM	finite element method
P&ID	piping and instrumentation diagram

References

[1] B. V. Smith, M. G. Ierapepritou, *Comput. Chem. Eng.* **2010**, *34 (6)*, 857–865. DOI: https://doi.org/10.1016/j.compchemeng.2010.02.039

[2] N. Kockmann, L. Bittorf, W. Krieger, F. Reichmann, M. Schmalenberg, S. Soboll, *Chem. Ing. Tech.* **2018**, *90 (11)*, 1806–1822. DOI: https://doi.org/10.1002/cite.201800020

[3] D. Reay, C. Ramshaw, A. Harvey, *Process Intensif.* **2013**, 205–249. DOI: https://doi.org/10.1016/B978-0-08-098304-2.00006-7

[4] A. Holbach, E. Çalişkan, H. S. Lee, N. Kockmann, *Chem. Eng. Process.* **2014**, *80*, 21–28. DOI: https://doi.org/10.1016/j.cep.2014.03.013

[5] D. Kreyenschulte, B. Heyman, A. Eggert, T. Maßmann, C. Kalvelage, R. Kossack, L. Regestein, A. Jupke, J. Büchs, *Biochem. Eng. J.* **2018**, *135*, 133–141. DOI: https://doi.org/10.1016/j.bej.2018.04.014

[6] J. Muendges, I. Stark, S. Mohammad, A. Górak, T. Zeiner, *Fluid Phase Equilib.* **2015**, *385*, 227–236. DOI: https://doi.org/10.1016/j.fluid.2014.10.034

[7] A. Keller, M. W. Hlawitschka, H.-J. Bart, *Sep. Purif. Technol.* **2021**, *275*, 119166. DOI: https://doi.org/10.1016/j.seppur.2021.119166

[8] M. Schmalenberg, T. A. Frede, C. Mathias, N. Kockmann, *Chem. Ing. Tech.* **2021**, *93 (3)*, 466–472. DOI: https://doi.org/10.1002/cite.202000066

[9] P. Sakthithasan, N. Gerdes, M. Venhuis, N. Kockmann, *Chem. Eng. Process.* **2022**, *180*, 108757. DOI: https://doi.org/10.1016/j.cep.2021.108757

[10] H.-J. Bart, C. Drumm, M. M. Attarakih, *Chem. Eng. Process.* **2008**, *47 (5)*, 745–754. DOI: https://doi.org/10.1016/j.cep.2007.11.005

[11] A. Baker, A. Fells, M. J. Carrott, C. J. Maher, B. C. Hanson, *Chem. Soc. Rev.* **2022**, *51 (10)*, 3964–3999. DOI: https://doi.org/10.1039/D2CS00192F

[12] C. Xu, T. Xie, *Ind. Eng. Chem. Res.* **2017**, *56 (27)*, 7593–7622. DOI: https://doi.org/10.1021/acs.iecr.7b01712

[13] P. Angeli, E. G. Ortega, D. Tsaoulidis, M. Earle, *Johnson Matthey Technol. Rev.* **2019**, *63 (4)*, 299–310. DOI: https://doi.org/10.1595/205651319X15669171624235

[14] A. Aota, M. Nonaka, A. Hibara, T. Kitamori, *Angew. Chem.* **2007**, *119 (6)*, 896–898. DOI: https://doi.org/10.1002/ange.200600122

[15] M. Polyakova, A. Diekmann, M. Grünewald, *Chem. Ing. Tech.* **2020**, *92 (12)*, 1941–1952. DOI: https://doi.org/10.1002/cite.202000081

[16] A. Fromme, F. Funke, J. Merz, G. Schembecker, *J. Chromatogr. A* **2020**, *1615*, 460742. DOI: https://doi.org/10.1016/j.chroma.2019.460742

[17] Development of a 9-cm annular centrifugal contactor, No. ANL-80-103, Argonne National Lab.(ANL), Argonne, IL (US) **1981**.

[18] D. H. Meikrantz, L. L. Macaluso, W. D. Flim, C. J. Heald, G. Mendoza, S. B. Meikrantz, *Chem. Eng. Commun.* **2002**, *189 (12)*, 1629–1639. DOI: https://doi.org/10.1080/00986440214582

[19] T. Míšek et al., *Standard Test Systems for Liquid Extraction*, Institution of Chemical Engineers, Rugby, UK **1985**.

[20] E. Grushka, E. J. Kikta, *J. Am. Chem. Soc.* **1976**, *98 (3)*, 643–648. DOI: https://doi.org/10.1021/ja00419a001

[21] M. Jamialahmadi, M. Emadi, H. Müller-Steinhagen, *J. Pet. Sci. Eng.* **2006**, *53 (1–2)*, 47–60. DOI: https://doi.org/10.1016/j.petrol.2006.01.011

[22] I. Wagner, J. Stichlmair, *Chem. Eng. Technol.* **2001**, *24 (6)*, 616–619. DOI: https://doi.org/10.1002/1521-4125(200106)24:6<616::AID-CEAT616>3.0.CO;2-T

[23] M. V. Rathnam, R. T. Sayed, K. R. Bhanushali, M. S. S. Kumar, *J. Chem. Eng. Data* **2012**, *57 (6)*, 1721–1727. DOI: https://doi.org/10.1021/je300085z

[24] S. Zeppieri, J. Rodríguez, A. L. López de Ramos, *J. Chem. Eng. Data* **2001**, *46 (5)*, 1086–1088. DOI: https://doi.org/10.1021/je000245r

[25] A. S. Michaels, E. A. Hauser, *J. Phys. Colloid Chem.* **1951**, *55 (3)*, 408–421. DOI: https://doi.org/10.1021/j150486a008

[26] G. Alvarez-Rivera, M. Bueno, D. Ballesteros-Vivas, J. A. Mendiola, E. Ibañez, *Pressurized Liquid Extraction Liquid-Phase Extraction*, Elsevier, Cambridge, MA **2020**, 375–398.

[27] L. C. Sander, *J. Res. Natl. Inst. Stand. Technol.* **2017**, *122 (7)*, 6028. DOI: https://doi.org/10.6028/jres.122.007

[28] A. Nieto, F. Borrull, E. Pocurull, R. M. Marcé, *Trends Anal. Chem.* **2010**, *29 (7)*, 752–764. DOI: https://doi.org/10.1016/j.trac.2010.03.014

[29] M. D. L. de Castro, J. L. L. García, in *High-pressure, high-temperature solvent extraction in Techniques and Instrumentation in Analytical Chemistry*, Vol. 24, 233–279, **2002**.

[30] B. Díaz-Reinoso, A. Moure, H. Domínguez, J. C. Parajó, *J. Agric. Food Chem.* **2006**, *54 (7)*, 2441–2469. DOI: https://doi.org/10.1021/jf052858j

[31] E. Reverchon, I. De Marco, *J. Supercrit. Fluids* **2006**, *38 (2)*, 146–166. DOI: https://doi.org/10.1016/j.supflu.2006.03.020

[32] C. Erkey, *J. Supercrit. Fluids* **2000**, *17 (3)*, 259–287. DOI: https://doi.org/10.1016/S0896-8446(99)00047-9

[33] T. Fujii, Y. Matsuo, S. Kawasaki, *Ind. Eng. Chem. Res.* **2018**, *57 (16)*, 5717–5721. DOI: https://doi.org/10.1021/acs.iecr.8b00812

[34] A. Pieck, C. Crampon, A. Fabien, E. Badens, *J. Supercrit. Fluids* **2022**, *179*, 105404. DOI: https://doi.org/10.1016/j.supflu.2021.105404

[35] G. Brunner, N. T. Machado, *J. Supercrit. Fluids* **2012**, *66*, 96–110. DOI: https://doi.org/10.1016/j.supflu.2012.02.012

[36] M. Roodpeyma, S. E. Guigard, W. H. Stiver, *J. Supercrit. Fluids* **2018**, *135*, 120–129. DOI: https://doi.org/10.1016/j.supflu.2017.12.029

[37] VDI 2220, *Product Planning; Flow, Terms and Organization*, VDI guideline, Verein Deutscher Ingenieure, Düsseldorf **1980**.

[38] VDI 2221, *Design of Technical Products and Systems – Model of Product Design*, VDI guideline, Verein Deutscher Ingenieure, Düsseldorf **1993**.

[39] Verein Deutscher Ingenieure (ed) (1997) VDI 2222 – Methodisches Entwickeln von Lösungsprinzipien. Beuth Verlag GmbH, Berlin/Düsseldorf.

[40] VDI 2223, *Systematic Embodiment Design of Technical Products*, VDI guideline, Verein Deutscher Ingenieure, Düsseldorf **2004**.

[41] *ASME Boiler and Pressure Vessel Code, Section VIII: Rules for Construction of Pressure Vessels, Division 1*, The American Society of Mechanical Engineers, New York **2021**.

[42] S. Soboll, N. Kockmann, *Chem. Eng. Technol.* **2018**, *41 (9)*, 1847–1856. DOI: https://doi.org/10.1002/ceat.201800283

[43] www.ansys.com/materials (Accessed on December 14, 2022)

[44] VDI 2230, *Systematic Calculation of Highly Stressed Bolted Joints – Joints with One Cylindrical Bolt*, VDI guideline, Verein Deutscher Ingenieure, Düsseldorf **2015**.

[45] P. Stephan, in *VDI-Wärmeatlas*, Springer, Berlin **2013**, Sect. B2, 23–36. DOI: https://doi.org/10.1007/978-3-642-19981-3_4

[46] M. Wagner, *Lineare und nichtlineare FEM*, Springer, Wiesbaden **2022**. DOI: https://doi.org/10.1007/978-3-658-36522-6

